Jamming transitions in force-based models for pedestrian dynamics

Mohcine Chraibi,[1,*] Takahiro Ezaki,[2] Antoine Tordeux,[1] Katsuhiro Nishinari,[3] Andreas Schadschneider,[4] and Armin Seyfried[1]

[1]*Jülich Supercomputing Centre, Forschungszentrum Jülich, 52425 Jülich, Germany*

[2]*Department of Aeronautics and Astronautics, Graduate School of Engineering, The University of Tokyo, 7-3-1, Hongo, Bunkyo-ku, Tokyo 113-8656, Japan*

[3]*Research Center for Advanced Science and Technology, The University of Tokyo, 4-6-1, Komaba, Meguro-ku, Tokyo 153-8904, Japan*

[4]*Institute for Theoretical Physics, Universität zu Köln, 50937 Köln, Germany*

(Received 8 December 2014; revised manuscript received 21 September 2015; published 12 October 2015)

Force-based models describe pedestrian dynamics in analogy to classical mechanics by a system of second order ordinary differential equations. By investigating the linear stability of two main classes of forces, parameter regions with unstable homogeneous states are identified. In this unstable regime it is then checked whether phase transitions or stop-and-go waves occur. Results based on numerical simulations show, however, that the investigated models lead to unrealistic behavior in the form of backwards moving pedestrians and overlapping. This is one reason why stop-and-go waves have not been observed in these models. The unrealistic behavior is not related to the numerical treatment of the dynamic equations but rather indicates an intrinsic problem of this model class. Identifying the underlying generic problems gives indications how to define models that do not show such unrealistic behavior. As an example we introduce a force-based model which produces realistic jam dynamics without the appearance of unrealistic negative speeds for empirical desired walking speeds.

DOI: 10.1103/PhysRevE.92.042809 PACS number(s): 89.40.−a, 45.70.Vn, 34.10.+x

I. INTRODUCTION

Mathematical models based on ideas from physics can improve our understanding of the characteristics of crowds and give useful insights into their dynamics. From a more practical point of view such models have applications, e.g., in safety analysis of large public events where they may help predicting critical situations, allowing preventive measures.

A popular class of models is of microscopic nature, describing the dynamics of crowds by specifying properties of individuals and defining their interactions. The most elaborated models belong either to the subclass of rule-based models that are discrete in space (i.e., cellular automata), or to force-based models continuous in space, which are described by a system of second order ordinary differential equations [1–4].

Especially for applications in safety analysis, models that are validated qualitatively and quantitatively are required. Quantitative validation of pedestrian dynamics consists of measuring density, velocity, and flow in simulations and comparing them with empirical data. The relation between these quantities, also called the fundamental diagram, is widely considered as the most important criterion to validate simulation results [5,6]. Besides this quantitative validation often the focus is more on the reproduction of qualitative properties, especially collective effects. Most of the force-based models are in fact able to describe fairly well some of those phenomena, e.g., lane formation [7,8], oscillations at bottlenecks [7,9], the "faster-is-slower" effect [10,11], and clogging at bottlenecks [8,9], that sometimes are difficult to verify empirically [12,13].

An often observed collective phenomenon that emerges in crowds, especially when the density exceeds a critical value, is stop-and-go waves [2]. Although some space-continuous models [14–17] reproduce partly this phenomenon, force-based models generally fail to describe pedestrian dynamics in jam situations correctly. Instead in some situations quite often unrealistic behavior like backward motion or overtaking ("tunneling") is observed, especially in one-dimensional single-file scenarios. Recently, it has been shown [18] that this is not a consequence of numerical problems in the treatment of the differential equations, but an indication of inherent problems of force-based models, at least for certain classes of forces.

In vehicular traffic, the formation of jams and the dynamics of traffic waves have been studied intensively [19–22]. Traffic jams in simulations occur as a result of phase transitions from a stable homogeneous configuration to an unstable configuration. That means it should be possible to calibrate model parameters such that systems in unstable regimes can be simulated. Otherwise, a reproduction of jams is impossible and the model can be qualified as unrealistic. For each parameter set that leads to an unstable homogeneous state it has to be verified by simulations whether this instability corresponds to realistic behavior (i.e., the occurrence of jams) or unrealistic behavior (e.g., overlapping of particles). A certain amount of overlapping might be acceptable as it could be interpreted as "elasticity" of the particles. Generically, however, the amount of overlapping is not limited in these models and even tunneling of particles is observed.

In pedestrian dynamics, numerous force-based models have been developed based on physical analogies, i.e., Newtonian dynamics. Pedestrian dynamics is described as a deviation from a predefined desired direction resulting from forces acting on each pedestrian. These forces are not fundamental physical forces, but effective forces that give a physical interpretation of the decisions made by pedestrians. Therefore, the forces cannot be measured directly but only via their effects on the motion, i.e., the observed accelerations. This might be one reason why in the literature a diversity of models has been proposed, e.g., based on algebraically decaying forces, exponential forces, etc. Although the force-based ansatz is elegant and to some extent

*m.chraibi@fz-juelich.de

helpful in describing the dynamics of pedestrians, it has some intrinsic problems that we will discuss in this paper. These problems were observed earlier and have lead to modifications of the original models by introducing additional forces, like a physical force, or even restrictions on the state variables.

Köster *et al.* [23] gave a thorough analysis of the numerical problems that are encountered when simulating pedestrian dynamics with force-based models. As shown in [23,24] the problem of oscillations in the trajectories of pedestrian (backwards movement) is an *intrinsic* problem of second order models, not (only) a numerical one due to the accuracy of the numerical solver. In [18] an analytical investigation of the social force model in one-dimensional space proved that oscillations can only be avoided by choosing values in some defined parameter spaces. Unfortunately, these parameter values are either unrealistic (if they have a physical meaning) or they lead to a large amount of overlapping (and in extreme cases, e.g., high densities, tunneling) of pedestrians. This so-called overlapping-oscillation duality is discussed in more detail in [25,26]. These problems, that often lead to a "complexification" of the original (elegant) ansatz of force-based models, may explain the paradigm shift observed lately with the emergence of improved first-order models or so-called "velocity models" [14,17,27–33].

In this work we introduce a classification of force-based models according to the form of the repulsive force. The stability properties of each class can be investigated separately in a unified way. Analytical criteria that ensure reproduction of stop-and-go waves in terms of the instability of uniform single-file motion are derived. Furthermore, we analyze the influence of specific parameters of the overall behavior of the investigated model. A focus is on the analytical forms of the models, and not on eventual numerical difficulties. Based on numerical simulations we show that the investigated models behave unrealistically in unstable regimes, which is manifested in negative speeds (movement in the opposite of the desired direction) and oscillations in position of pedestrians (leads to nonphysical overlapping). After identifying the origin of this unrealistic behavior we attempt to develop a model that mitigates these problems. We observe that this model shows phase separation in its unstable regime, in agreement with empirical results [34]. We conclude with a discussion of the results and analysis of their consequences as well as a detailed discussion of the limitation of the proposed model in special and force-based models in general.

II. MODEL DEFINITION

Pedestrian dynamics is generically a two-dimensional problem. In order to reduce the complexity and to capture the essentials of the jamming dynamics, we focus here on 1D systems. Furthermore we assume an asymmetric nearest-neighbor interaction where the motion of a pedestrian is only influenced by the person immediately in front. N pedestrians are initially distributed uniformly in a one-dimensional space with periodic boundary conditions. Important information can then be derived from the reaction of the system in the uniform steady state to small perturbations.

For the state variables position x_n and velocity $\dot{x}_n = \frac{dx_n}{dt}$ of pedestrian n we define the distance of the centers Δx_n and the relative velocity $\Delta\dot{x}_n$ of two successive pedestrians, respectively, as (see Fig. 1)

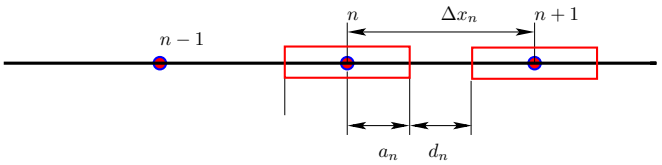

FIG. 1. (Color online) Definition of the quantities characterizing the single-file motion of pedestrians (represented by rectangles).

$$\Delta x_n = x_{n+1} - x_n, \quad \Delta\dot{x}_n = \dot{x}_{n+1} - \dot{x}_n. \tag{1}$$

For convenience, we will mainly use dimensionless quantities in the following. These are defined by the transformation

$$t \to t' = \frac{t}{\tau} \quad \text{and} \quad x_n \to x_n' = \frac{x_n}{a_0}, \tag{2}$$

with time constant τ and the length constant a_0. To simplify the notation we denote the rescaled velocity by $\dot{x}_n' = dx_n'/dt'$.

In general, pedestrians are modeled as simple geometric objects of constant size, e.g., a circle or ellipse. In one-dimensional space the size of pedestrians is characterized by a_n (Fig. 1), i.e., their length is $2a_n$. However, it is well known that the space requirement of a pedestrian depends on its velocity and is defined in a general way as a linear function of the velocity [35]

$$a_n = a_0 + a_v\dot{x}_n. \tag{3}$$

In the following, the parameter a_0, characterizing the space requirement of a standing person, will be used as length scale for the dimensionless quantities (2). Note that the parameter $a_v \geqslant 0$ has the dimension of time. The dimensionless spacing $a_n' = a_n/a_0$ is written as

$$a_n' = 1 + \tilde{a}_v\dot{x}_n', \quad \text{with} \quad \tilde{a}_v = \frac{a_v}{\tau}. \tag{4}$$

The effective distance (distance gap) d_n of two consecutive pedestrians becomes in dimensionless form

$$d_n' = \frac{d_n}{a_0} = \Delta x_n' - a_n' - a_{n+1}' = \Delta x_n' - \tilde{a}_v(\dot{x}_n' + \dot{x}_{n+1}') - 2. \tag{5}$$

The dynamical equation of force-based models is usually defined as the superposition of a repulsive force f and a driving term g [36]. The driving term is of central importance and the standard form used is

$$g(\dot{x}_n) = \frac{v_0 - \dot{x}_n}{\tau}. \tag{6}$$

Typical values for the parameters are $\tau = 0.5$ s for the relaxation time and $v_0 = 1.2$ m/s for the desired speed. Note that τ is the same time scale used in Eq. (2). This definition gives rise to exponential acceleration to v_0 in free-flow movement. The equation of motion for pedestrian n has the generic form

$$\ddot{x}_n = f(\dot{x}_n, \Delta\dot{x}_n, \Delta x_n) + g(\dot{x}_n)\cdot \tag{7}$$

In this work we limit ourselves to models that incorporate (6) as driving term and investigate the stability of several force-based models, defined through different functions $f(\cdot)$ corresponding to repulsive forces that either decay algebraically or exponentially with distance. We consider unidimensional dynamics and totally asymmetric interaction with the predecessor and assume that the repulsive forces are negative. We determine their instability regions where the investigated model may be able to reproduce stop-and-go waves. Technical details of the stability analysis, which is a standard tool that can lead to cumbersome calculations, are deferred to the Appendix which provides all relevant results.

III. MODELS WITH ALGEBRAICALLY DECAYING FORCES

In this section we consider force-based models with an algebraically decaying repulsive term, i.e.,

$$f(\dot{x}_n, \Delta\dot{x}_n, \Delta x_n) \propto 1/(d_n)^q. \tag{8}$$

More specifically, we consider the following dimensionless equation of motion:

$$\ddot{x}'_n = -\frac{(\mu + \delta \cdot r_\varepsilon(\Delta\dot{x}'_n))^2}{{d'_n}^q} + v'_0 - \dot{x}'_n, \tag{9}$$

with a dimensionless parameter $\mu \geqslant 0$ to adjust the strength of the force, the dimensionless desired speed $v'_0 = \frac{v_0\tau}{a_0} > 0$, and constants $\delta \geqslant 0$ and $q > 0$. In two-dimensional space the case $q < 1$ corresponds to a long-ranged repulsive force, whereas the force is short ranged for $q > 1$. Note that the definition of the model implies that each pedestrian only interacts with its predecessor. Equation (9) can be interpreted as an extension of the generalized centrifugal force model [25] which corresponds to the special case $\delta = 1$. The differentiable function,

$$r_\varepsilon(x) = \varepsilon \, \log(1 + e^{-x/\varepsilon}) \quad (0 < \varepsilon \ll 1), \tag{10}$$

is an approximation of the nondifferentiable ramp function

$$r(x) = \begin{cases} 0, & x \geqslant 0, \\ -x, & \text{else}, \end{cases} \tag{11}$$

as $\varepsilon \to 0$ (see Fig. 2). This function suppresses the repulsive effect of a predecessor moving faster than the follower. (We will set $\varepsilon = 0.1$ in the simulations.)

A. Model classification

The model class defined by Eq. (9) depends on four (dimensionless) parameters μ, δ, q, and $\tilde{a}_v$ [which enters via (5)] and includes several models studied previously. In the following each model will by specified by the quadruple $\mathcal{Q} = \langle \mu, \delta, q, \tilde{a}_v \rangle$. As we will see later the parameters δ and $\tilde{a}_v$ are most critical for the dynamics described by Eq. (9). The parameter δ controls the influence of the relative velocity, whereas $\tilde{a}_v$ determines the velocity dependence of the effective size of the pedestrians. Although in principle δ can be any real number, in most known models it takes only discrete values in $\{0,1\}$.

In the centrifugal force model (CFM) [8] the size of the pedestrians is independent of their speed. In addition, the CFM considers the effects of the relative velocity $\Delta\dot{x}_n$, such that slow pedestrians are not effected by faster ones. Hence we can define the CFM as $\mathcal{Q} = \langle 0,1,1,0 \rangle$. In contrast to the CFM, the generalized centrifugal force model (GCFM) [25] includes both components—the relative velocity and the velocity dependence of the volume exclusion [37]. Additionally, to avoid overlapping of pedestrians that results from repulsive forces among pedestrians that are too small, moving *nearly* in lockstep, a non-negative constant μ is added to the relative velocity. Thus the GCFM corresponds to the case $\mathcal{Q} = \langle \mu, 1, 1, \tilde{a}_v \rangle$.

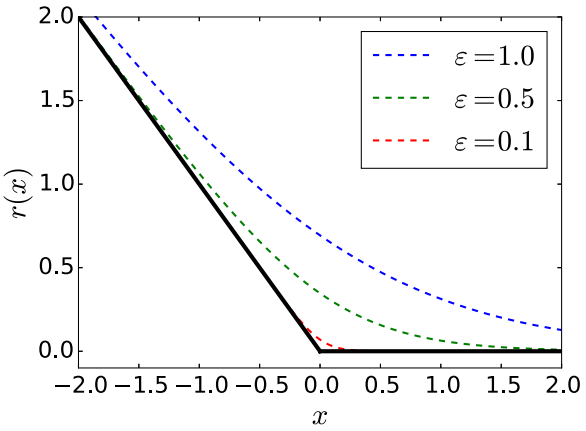

FIG. 2. (Color online) Approximations $r_\varepsilon(\cdot)$ of the ramp function $r(\cdot)$ (thick line). In the simulations we use $\varepsilon = 0.1$.

Another model that represents pedestrians with constant circles and thus has $\tilde{a}_v = 0$ was introduced in Ref. [38] which we will refer to as HFV (Helbing, Farkas, and Vicsek). Different to the CFM and GCFM, in HFV the effects of the relative velocity are ignored so that the HFV can be characterized by $\mathcal{Q} = \langle \mu, 0, 2, 0 \rangle$. In Ref. [39] an enhancement of the HFV was introduced by Seyfried *et al.* (SEY) consisting on a velocity-dependent space requirement, i.e., $\mathcal{Q} = \langle \mu \neq 0, 0, 2, \tilde{a}_v \neq 0 \rangle$. Furthermore, in Refs. [40,41] Guo *et al.* investigated a slightly different model (GUO) with the focus on navigation in two-dimensional space. The GUO model can be classified as $\mathcal{Q} = \langle \mu, 0, 1, 0 \rangle$. Similar models introducing new features have been proposed in Refs. [42] and [43] with a constant added to the denominator of $f(\cdot)$. They correspond to the case $\mathcal{Q} = \langle \mu, 0, 2, 0 \rangle$.

In Table I a brief summary of the aforementioned models is given.

Some force-based model rely on additional algorithmic solutions like collision detection techniques [8] or a

TABLE I. $\mathcal{Q}$ values of the investigated models with algebraically decaying forces.

Model	$\mathcal{Q} = \langle \mu, \delta, q, \tilde{a}_v \rangle$
CFM	$\langle 0,1,1,0 \rangle$
GCFM	$\langle \mu,1,1,\tilde{a}_v \rangle$
HFV	$\langle \mu,0,2,0 \rangle$
SEY	$\langle \mu,0,2,\tilde{a}_v \rangle$
GUO	$\langle \mu,0,1,0 \rangle$

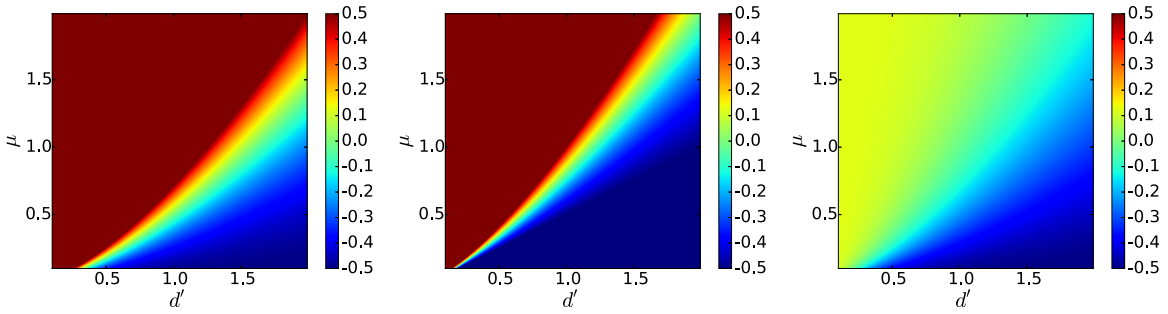

FIG. 3. (Color online) Stability region of the algebraically decaying models with respect to μ and d'. Left: $\mathcal{Q} = \langle \mu,0,2,0 \rangle$. Middle: $\mathcal{Q} = \langle \mu,1,2,0 \rangle$. Right: $\mathcal{Q} = \langle \mu,0,2,0.2 \rangle$. The colors are mapped to the value of Φ in Eq. (17). Negative values of Φ indicate stability regions.

time-to-collision constant [44] that allows one to manage collisions in simulations. Other models rely on optimization algorithms to define the desired direction of pedestrians [45] depending on the situation of every pedestrian in the simulation. While these additional components may prove to be useful for numerical simulations, they have the downside of adding more complexity to the model while stretching the concept of force-based modeling beyond the original idea. In some models, e.g. [44], these components are strongly correlated with the forces, which complicates the analytical investigation of the "pure" force model. Therefore, in this paper the analytical investigation is limited solely to the force-based models that can be formulated without any additional algorithmic components.

B. Linear stability

We study the linear stability of the system (9) for a given set $\mathcal{Q}$ of parameters. The positions of the pedestrians in the homogeneous steady state are given by

$$y_n = \frac{1}{a_0}\left(\frac{n}{\rho} + vt\right), \tag{12}$$

so that $y_{n+1} - y_n = \frac{1}{a_0\rho} = \Delta y$, $\dot{y}_n = v\tau/a_0 = v'$, and $\ddot{y}_n = 0$ for all n, where derivatives are taken with respect to t'. Now we consider small (dimensionless) perturbations ϵ_n of the steady state positions,

$$x_n' = y_n + \epsilon_n. \tag{13}$$

For perturbations of the form

$$\epsilon_n(t) = \alpha_n e^{zt}, \tag{14}$$

with $\alpha_n, z \in \mathbb{C}$ we then find (expanding to first order)

$$z^2 = \delta\gamma \frac{e^{ik} - 1}{d'^q} z - \phi\tilde{a}_v(e^{ik} + 1)z + \phi(e^{ik} - 1) - z, \tag{15}$$

with $\gamma = \mu + \delta\varepsilon \log(2)$, $\phi = \frac{q\gamma^2}{d'^{q+1}}$, and $k = 2\pi l/N$ with $l = 0, \ldots, N-1$. Details of the derivation can be found in the Appendix, Sec. A 1.

For $k \approx 0$ we can expand z as a polynomial in k:

$$z = z^{(0)}k + z^{(1)}k^2 + \cdots. \tag{16}$$

Up to second order we then find the stability condition (see Appendix, Sec. A 1 a)

$$\gamma > 0, \quad \Phi := \phi\omega - \frac{\delta\gamma}{d'^q} - \tfrac{1}{2} < 0. \tag{17}$$

Here $d' = \Delta y - 2\tilde{a}_v v - 2$, with $\tilde{a}_v = a_v/\tau$ and $\omega = 1/(2\tilde{a}_v\phi + 1)$. The stability condition (17) suggests that models of type $\mathcal{Q} = \langle \mu \neq 0,0,q,0 \rangle$, e.g., the HFV, GUO models, tend to instability with increasing density and increasing strength of the force (μ), because Φ simplifies to $\phi - \frac{1}{2}$. Adding the influence of the relative speed ($\delta \neq 0$) leads to a comparable structure (compare Fig. 3, left and middle).

Modifying these models by introducing a velocity-dependent enlargement of pedestrians, i.e., considering models in class $\mathcal{Q} = \langle \mu \neq 0,0,q,\tilde{a}_v \neq 0 \rangle$, leads to $\Phi = \phi\omega - \frac{1}{2}$, with smaller ω by increasing $\tilde{a}_v$, which has a stabilizing effect on the system (see Fig. 3, right). This means the velocity dependence in this kind of models enhances the stability of the system. In comparison, the impact of the relative velocity on the stability of the system is less significant.

Inverting the sign of δ adds a positive term to $\phi\omega^2$ in the expression of Φ, which increases the instability of the system. Although negative values of δ give rise to instabilities, they are physically not relevant, since that would imply that a faster pedestrian in front has more influence on a slower pedestrian directly behind.

C. Simulations

We solve the system of equations (9) for $N = 67$ using Heun's scheme with time step $\Delta t = 10^{-5}$ s. According to [46] Heun's scheme seems to be the best scheme for simulations of pedestrian dynamics for many practical scenarios. For all simulations performed in this work we use this scheme with an unchanged Δt.

Pedestrians are uniformly distributed in a one-dimensional system with periodic boundary conditions and length $L = 200$ m. The chosen values of N and L lead to $d' \approx 1$ ($\tilde{a}_v = 0$). $v_0' = 3$. The initial velocities are set to zero. The maximum simulation time is $\Delta t = 2000$ s. Only the initial position of the first pedestrian is slightly perturbed, i.e., $\epsilon_1 = 10^{-4}$ ($\epsilon_{n\neq 1} = 0$).

With $\Phi = 0$ in Eq. (A24) we obtain for $\delta = \tilde{a}_v = 0$ the critical value for μ as $\mu_{\mathrm{cr}} = \sqrt{\frac{d'^{q+1}}{2q}}$. Therefore, a model of type $\mathcal{Q} = \langle 0.45,0,2,0 \rangle$ is stable since $\mu = 0.45$ is smaller than this critical value $\mu_{\mathrm{cr}} = \frac{1}{2}$.

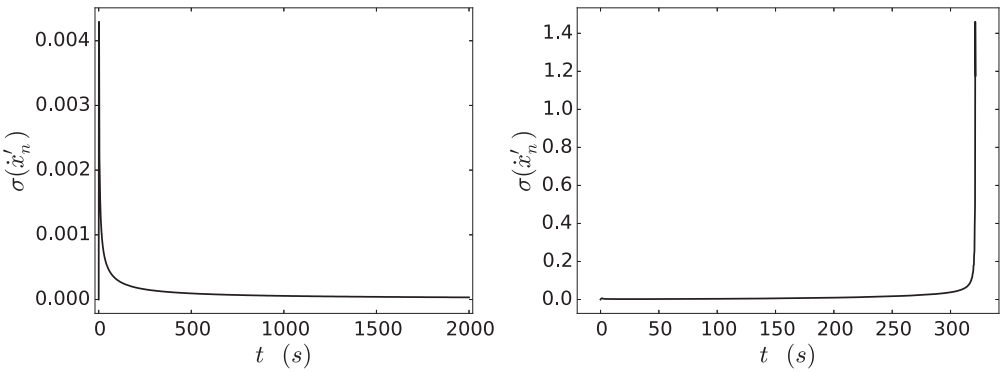

FIG. 4. Standard deviation of the speeds with respect to simulation time. The initial perturbation in the speed disperses to zero when the system is stable (left: $\mu = 0.45$), while it grows when the system is unstable (right with $\mu = 0.55$).

To observe the behavior of the system in the unstable regime we perform simulations for a parameter set $\mathcal{Q} = \langle 0.55,0,2,0\rangle$ with $\mu > \mu_{\rm cr}$. The simulations show an oscillatory behavior that leads inevitably to overlapping among pedestrians. Note that the model is not defined when the distance d' is zero; see Eq. (9). This phenomenon (overlapping) is a stopping criterion for the simulation.

Since all pedestrians start with speed zero and due to the small perturbation of the initial position (ϵ_1) the speeds of pedestrians in the beginning of simulations are perturbed too. However, depending on the state of the system this initial perturbation may disperse to zero if the system is stable. Otherwise, it will grow until the simulation is stopped due to overlapping. Figure 4 shows a comparison between the time evolution of the speed's standard deviation for both cases $\mathcal{Q} = \langle 0.45,0,2,0\rangle$ and $\mathcal{Q} = \langle 0.55,0,2,0\rangle$.

We conclude that in the unstable regime the investigated models with algebraic forces lead to negative velocities (backward movement) and hence unrealistic behavior. Introducing a velocity-dependent enlargement of pedestrians stabilizes the system, but the unstable regime remains unrealistic since the volume exclusion of a pedestrian (a'_n) with a negative speed can become negative.

IV. EXPONENTIAL-DISTANCE MODELS

In this section we consider models with

$$f(\dot{x}_n, \Delta x_n) \propto \exp(-d'_n), \tag{18}$$

i.e., exponentially decaying repulsive forces using use the notation introduced in the previous section.

The paradigmatic model in this class is arguably the social force model (SFM) as originally introduced in [47]. Further modifications and enhancements followed. In [48] a physical force was introduced to mitigate overlapping among pedestrians. Lakoba *et al.* [10] studied the calibration of the modified SFM by improving the numerical efficiency of the model and introducing several enhancements. The calibration of the modified SFM was investigated again in [49] by means of an evolutionary optimization algorithm. Parisi *et al.* [50] investigated the difficulties of SFM concerning quantitative description of pedestrian dynamics by introducing a mechanism, called "respect mechanism" to mitigate overlapping among pedestrians. Finally, in Ref. [51] an interesting ansatz to calibrate the SFM by means of experimental measurements led to a modified repulsive force that includes the effect of the distance as well as the angle between two pedestrians. However, these measurements, basically from experiments with two pedestrians, are extrapolated to a crowd with several individuals. Hence it implicitly assumes that the superposition of forces can be applied. This hypothesis, however, lacks experimental evidence in the context of pedestrian dynamics. Often different specifications of the repulsive force are adopted, in the form of circular or elliptical equipotential lines. However, for a one-dimensional analysis both specifications are equivalent. In comparison to the models with algebraic forces the exponential force has no singularity at $d' = 0$. Hence it is defined for all distances and no regularization is required.

A. Linear stability

One common point among the aforementioned models is their consideration of a "physical" force to mitigate overlapping among pedestrians. For the stability analysis we therefore consider the following system using dimensionless variables:

$$\ddot{x}'_n = -a\, \exp\left(-\frac{d'_n}{b}\right) - c\, r_\varepsilon(d'_n) + v'_0 - \dot{x}'_n, \tag{19}$$

with a, b, and c dimensionless positive constants, d'_n as defined in (5), $v'_0 = \frac{v_0\tau}{a_0}$, and $r_\varepsilon(\cdot)$ the function (10).

The general form of these models contains five parameters. However, the value for τ was determined empirically in [51,52]. That means the system (19) can be defined by the quadruple

$$\tilde{\mathcal{Q}} = \langle a,b,c,\tilde{a}_v\rangle. \tag{20}$$

Similarly to Sec. III B we consider the effect of small perturbations $\epsilon_n(t) = \alpha_n e^{zt}$ to the steady state positions y_n. After some calculations outlined in the Appendix Sec. A 2 we obtain the following stability condition

$$\tilde{\Phi} := -\tfrac{1}{2} + \tilde{c}\alpha < 0, \tag{21}$$

with $\alpha = \frac{1}{2\tilde{b}-1}$, $\tilde{b} = \tilde{a}_v\tilde{c}$, $\tilde{c} = \tilde{a}/b - \frac{1}{2}c$, and $\tilde{a} = -a\exp(-d'/b)$.

Assuming d' is positive, which means $r_\varepsilon(\cdot)$ vanishes or simply $c = 0$, and the enlargement of pedestrians is constant

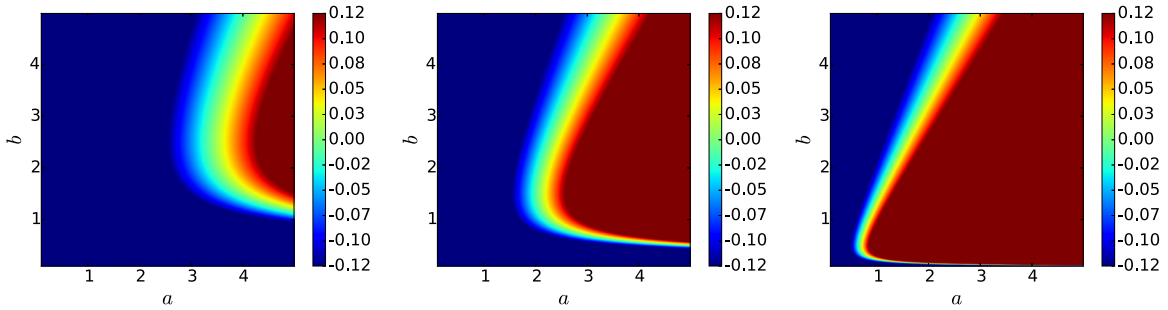

FIG. 5. (Color online) Stability region of a modified SFM ($\tilde{\mathcal{Q}} = \langle a,b,0,0\rangle$) with respect to a and b for different densities. Left: $d' = 2.5$. Middle: $d' = 1.5$. Right: $d' = 0.5$. The colors are mapped to the values of $\tilde{\Phi}$ [Eq. (23)]. Negative values indicate stability regions.

($\tilde{a}_v = 0$), we obtain

$$\tilde{b} = 0, \quad \alpha = -1, \tag{22}$$

and

$$\tilde{\Phi} = -\frac{1}{2} + \frac{a}{b}\exp(-d'/b). \tag{23}$$

Figure 5 depicts the stability regions for the $\tilde{\mathcal{Q}} = \langle a,b,0,0\rangle$-class models in the (a, b)-plane.

To investigate the effect of a velocity-dependent enlargement of pedestrians we evaluate the stability regions of $\tilde{\mathcal{Q}} = \langle 4,b,0,\tilde{a}_v\rangle$-class models. The value of $a = 4$ is according to Fig. 5 large enough to lay in an unstable region.

In Fig. 6 we observe that a system with a velocity-dependent enlargement ($\tilde{a}_v \neq 0$) becomes increasingly stable in the $(\tilde{a},b)$ space with decreasing density. This confirms the observation made in the previous section: velocity-dependent enlargement of pedestrians has a stabilizing effect on the system.

B. Simulations

Similar to Sec. III C we perform simulations with the exponential-distance models for different parameters. The same initial values and parameters as in Sec. III C are considered. $N = 57$ pedestrians are uniformly distributed, which corresponds to $d' \approx 1.5$.

For $a_v = c = 0$, the critical value of a in dependence of b is given by $a_{\mathrm{cr}} = \frac{b}{2\exp(-d'/b)}$. Accordingly, we choose $b = 1.5$ and $a = 3$, which yield an unstable system (compare also to Fig. 5).

Here again we make the same observation as with algebraically decaying models (Sec. III C). In the unstable regime a $\tilde{\mathcal{Q}} = \langle a,b,0,0\rangle$ models behave unrealistically. Instead of jams, collisions occur. Based on the time series of the speed's standard deviation, we compare the behavior of the model in a stable and an unstable regime [defined according to Eq. (21)]. Figure 7, left, shows as expected for $\tilde{\mathcal{Q}} = \langle 1.5,1.5,0,0\rangle$ that the standard deviation of the speed decreases to zero and the overall system converges to an homogeneous state, whereas it grows until the simulation interruption ($\tilde{\mathcal{Q}} = \langle 3,1.5,0,0\rangle$).

V. MODEL

In the previous sections we investigated properties of several force-based models related to jam formation. The linear stability analysis of these models yields conditions that determine parameter regions where unstable behavior may lead to stop-and-go waves in one-dimensional systems with boundary conditions. However, simulations with parameters in the unstable regime lead to unrealistic behavior (collisions, overlapping etc.) instead of stop-and-go waves. In this section we discuss the reasons for this failure and formulate a model that produces stop-and-go waves in its unstable regime.

Rewriting the generic equation of motion (7) as

$$\ddot{x}_n = \frac{\tilde{v}_0 - \dot{x}_n}{\tau}, \tag{24}$$

with $\tilde{v}_0 = \tau f + v_0 \leqslant v_0$ implies that the movement of pedestrian n is determined by a driving force with a modified and density-dependent desired speed $\tilde{v}_0$: the higher the density, the smaller the desired speed. However, if the desired speed is negative, which means pedestrians move backwards after some delay, collisions are likely to happen. This is in fact the case in the reciprocal-distance and exponential-distance models, where collisions are observed in the unstable regimes instead of jams.

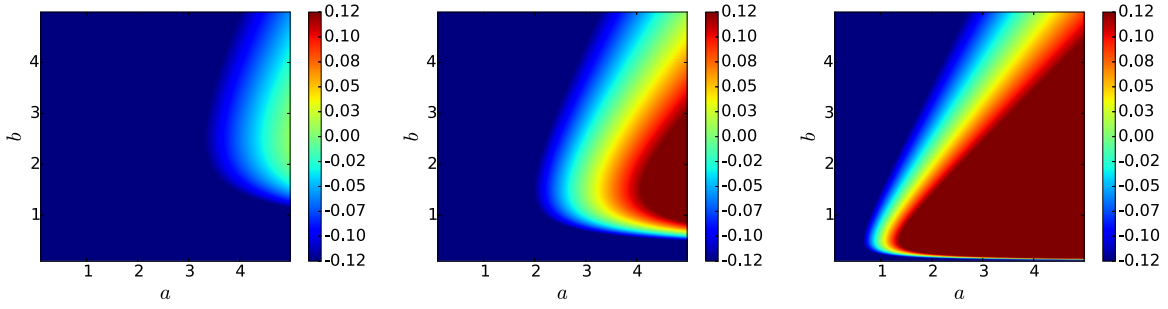

FIG. 6. (Color online) Stability region of a modified SFM ($\tilde{\mathcal{Q}} = \langle a,b,0,\tilde{a}_v = 0.15\rangle$) with respect to a and b for different densities. Left: $d' = 2.5$. Middle: $d' = 1.5$. Right: $d' = 0.5$.

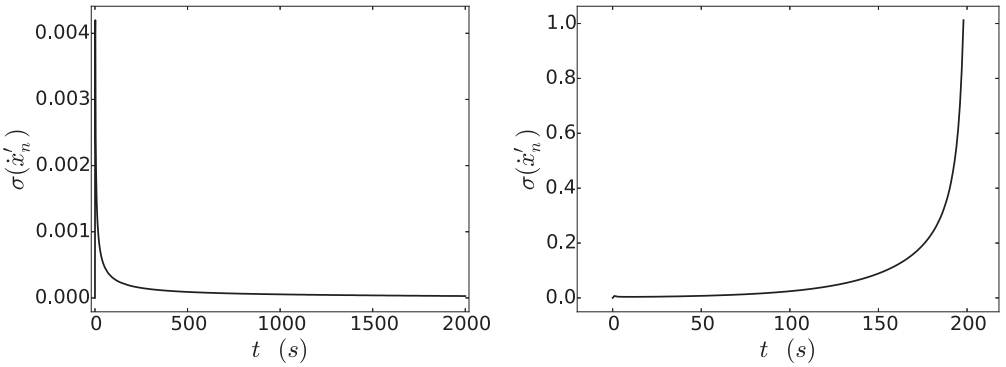

FIG. 7. Standard deviation of the speeds with respect to simulation time. The initial perturbation in the speed disperses to zero when the system is stable (left: $a = 1.5$, $b = 1.5$), while it grows when the system is unstable (right with $a = 3.0$, $b = 1.5$).

In order to avoid such problems, a nonlinear function $f(\Delta x_n, \dot{x}_n, \dot{x}_{n+1})$ such that $f(0,0,0) = -v_0/\tau$ is required. That means that overlapping of pedestrians leads to a vanishing desired speed $\tilde{v}_0 = 0$ instead of a negative one. Note that initial high values of v_0 may still lead to backward movement even if the resulting desired speed $\tilde{v}_0 = 0$. We discuss this effect in more detail in Sec. VI.

For f we propose the following expression:

$$f(\Delta x_n, \dot{x}_n, \dot{x}_{n+1}) = -\frac{v_0}{\tau} \log(c \cdot R_n + 1), \tag{25}$$

with

$$R_n = r_\varepsilon\left(\frac{\Delta x_n}{a_n + a_{n+1}} - 1\right), \quad c = e - 1. \tag{26}$$

Pedestrians anticipate collisions when their distance to their predecessors is smaller than a critical distance $a = a_n + a_{n+1}$, which is given by the addition of safety distances of two consecutive pedestrians. It is worth pointing out at this point that a_n does not model the body of pedestrian n but represents a "personal" safety distance. For $\Delta x_n = 0$, i.e., $R_n = 1$, the repulsive force reaches the value $-v_0/\tau$ to nullify the effects of the driving term (Fig. 8). In other words, the desired speed $\tilde{v}_0$ vanishes and pedestrians are not pushed to move *backwards*.

The corresponding dimensionless model we henceforth use is

$$\ddot{x}'_n = -v'_0 \ln(c \cdot R'_n + 1) - \dot{x}'_n + v'_0, \tag{27}$$

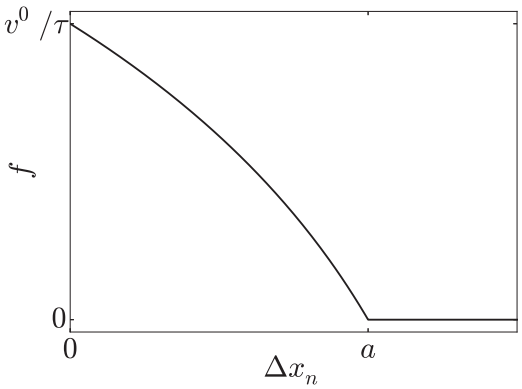

FIG. 8. Absolute value of the repulsive force according to Eq. (25).

with

$$R'_n = r_\varepsilon\left(\frac{\Delta x'_n}{a'_n + a'_{n+1}} - 1\right), \quad v'_0 = \frac{v_0 \tau}{a_0}. \tag{28}$$

The main difference between this model and the optimal velocity model [53,54] is the velocity-dependent space requirement of pedestrians, expressed by the critical distance a.

A. Stability analysis

In this section, we investigate the stability of this model. We suppose that $\Delta y < a'$, with $\Delta y = \frac{1}{\rho a_0}$ is the mean dimensionless spacing and $a' = 2(1 + \tilde{a}_v v')$, v' being the dimensionless speed for the equilibrium of uniform solution, and add a small perturbation ϵ_n to the dimensionless coordinates of pedestrians. For R'_n we obtain with $a' = 2(1 + \tilde{a}_v v')$ and $a'_v = \frac{\tilde{a}_v}{a'}$

$$R'_n \approx 1 - \frac{\Delta x'_n}{a'}(1 - a'_v(\dot{\epsilon}_n + \dot{\epsilon}_{n+1})). \tag{29}$$

From the equation of motion (27) we obtain with $d_0 = 1 + c(1 - \frac{\Delta y}{a'})$

$$\ln(c \cdot R'_n + 1) \approx \ln(d_0) + \frac{c}{d_0}\left(\frac{\Delta y}{a'} a'_v(\dot{\epsilon}_n + \dot{\epsilon}_{n+1}) - \frac{\Delta \epsilon_n}{a'}\right).$$

Equation (27) in steady state yields $v'_0 \ln(d_0) = v'_0 - v'$; thus

$$\ddot{\epsilon}_n = -v'_0 \frac{c}{d_0}\left(\frac{\Delta y}{a'} a'_v(\dot{\epsilon}_n + \dot{\epsilon}_{n+1}) - \frac{\Delta \epsilon_n}{a'}\right) - \dot{\epsilon}_n. \tag{30}$$

Equation (30) rewritten in the z domain yields

$$z^2 + (\xi a'_v \Delta y(e^{ik} + 1) + 1)z - \xi(e^{ik} - 1) = 0, \tag{31}$$

with $\xi = \frac{c v'_0}{a' d_0}$. Given $\hat{z}^{\pm}$ two solutions of (31) we show in Fig. 9 the influence of the velocity dependence of the safety distance ($\tilde{a}_v$) and the constant v'_0 on the stability behavior of the model.

As expected we observe that velocity-dependent safety distance has a stabilizing effect on the model. Unlike the previous models for $a_v \neq 0$ the model still can show significant unstable behavior. This observation is important since it has been shown in the context of different force-based models that constant space requirement of pedestrians is responsible for an unrealistic shape of the fundamental diagram in single-lane

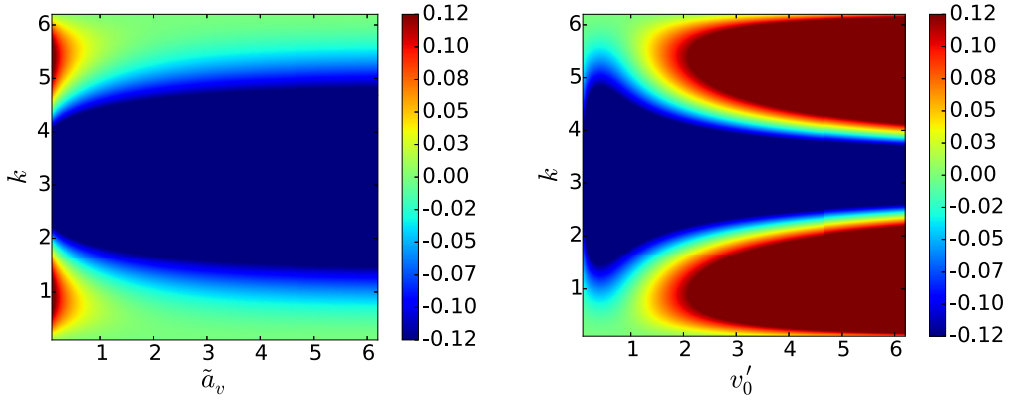

FIG. 9. (Color online) Left: stability region in the $(\tilde{a}_v,k)$ space for $v_0' = 3$ and $\Delta y = 1.5$. Right: stability region in the $(\tilde{v}_0',k)$ space for $\tilde{a}_v = 0$ and $\Delta y = 1.5$. The colors are mapped to the values of the real part of the positive solutions $\hat{z}^+$.

movement [25,39]. Additionally, we observe that increasing v_0' leads to an unstable system.

Expanding Eq. (31) around $k \approx 0$ yields the stability condition

$$\hat{\Phi} := \left(\frac{1}{1+2\xi a_v' \Delta y}\right)\left(\frac{\xi}{1+2\xi a_v' \Delta y} + \xi a_v' \Delta y\right) - 1/2 < 0. \tag{32}$$

For $\tilde{a}_v = 0$ the equation above simplifies to

$$\xi < 1/2, \quad \xi = \frac{c v_0'}{a' d_0}. \tag{33}$$

This result is in agreement with the stability condition $V' < 1/(2\tau)$ given in Ref. [53] for the system

$$\ddot{x}_n = A(V(\Delta x_n) - \dot{x}), \tag{34}$$

with $A = 1/\tau$ and $V(\Delta x_n) = v_0(1 - \ln(1 + cR))$.

The dimensionless from of the equation of motion (27) has only two free parameters, v_0' and $\tilde{a}_v$. In Fig. 10 we observe that the system becomes increasingly unstable with increasing v_0' (by a relatively small and constant $\tilde{a}_v$). Assuming that the free flow speed v_0 is constant, this means that increasing the reaction time τ or diminishing the safety space leads to unstable behavior of the system.

B. Simulations

We perform simulations with the introduced models using the same setup as before. For $\tilde{a}_v = 0$, $v_0' = 1$, and $\Delta y_n = 1.5$ we calculate the solution for 3000 s. Figure 11 shows the trajectories of 133 pedestrians. ε in Eq. (26) is set to 0.01.

As shown in Fig. 12 the speed does not become negative, therefore backward movement is not observed. This condition favors the appearance of stable jams.

Figure 13 shows the time evolution of the speed's standard deviation. After a relatively pronounced increase of the standard deviation, a stable plateau is formed. That means the system is in a "stable" homogeneous state.

VI. DISCUSSION AND SUMMARY

Since their first application to pedestrian dynamics by Hirai and Tarui [55], force-based models have been used extensively to investigate the properties of crowds. The "goodness" of these models is usually asserted by means of qualitative and/or quantitative investigations. Hereby, a model is judged to be realistic if its description of pedestrian dynamics is consistent with empirical findings. As an example, the fundamental diagram is often used as a benchmark to test the plausibility of such models.

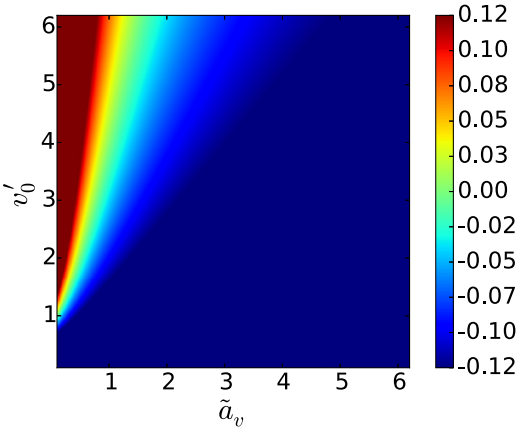

FIG. 10. (Color online) Stability region in the $(\tilde{a}_v,v_0')$ space for $\Delta y = 1.5$. The colors are mapped to the values of $\hat{\Phi}$ in Eq. (32).

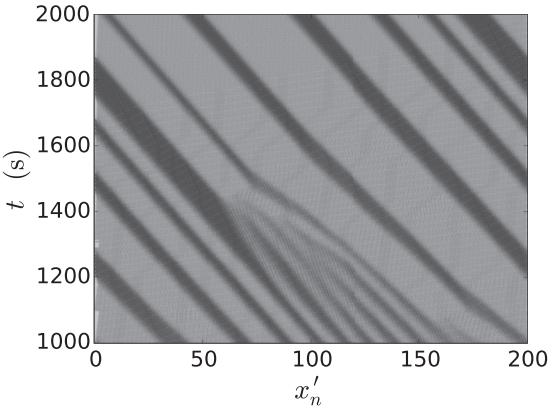

FIG. 11. Trajectories by $\Delta y_n = 1.5$. The trajectories show stop-and-go waves.

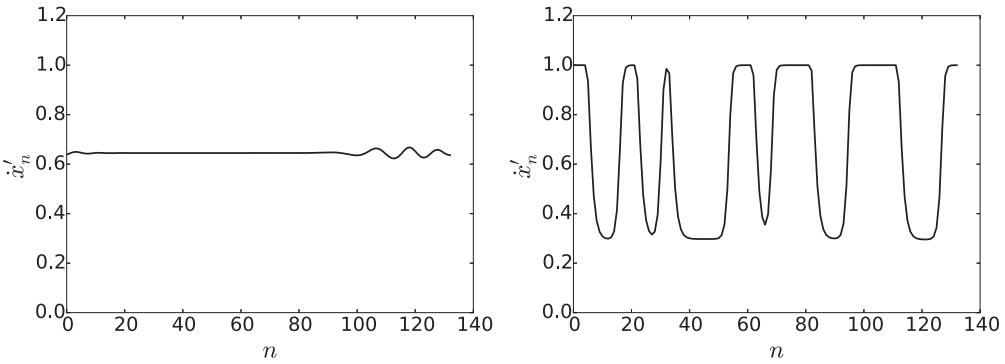

FIG. 12. Speed of pedestrians at different time steps. Left: $t = 300$ s; right: $t = 2000$ s.

Depending on the expression of the repulsive force, we classify the investigated force-based models as "algebraically decaying" and "exponential-distance models." The repulsive force in the first category is inversely proportional to the effective distance of two pedestrians [8,25,38–43]. In the second category, however, the magnitude of the repulsive force increases exponentially with decreasing distance [10,47–51]. Hybrid models that rely on additional mechanisms to optimize the desired direction of pedestrians (e.g. [45]) or to handle collisions among pedestrians like for example [44,56], where the concept of the time-to-collision is incorporated in the repulsive forces, make the analytic form of the repulsive force way too complicated to be investigated analytically. Therefore, we do not include these models in our analysis.

In this work we apply a method that gives insights into the characteristics of force-based models for pedestrian dynamics. It is based on an analytical approach by investigating the linear stability of the homogeneous steady state. In this manner, it is possible to determine for which parameter set, if any exists, a model is able to reproduce inhomogeneous states. Yet the nature of the unstable states (and the presence of realistic stop-and-go waves) has to be described by simulation. From an empirical point of view, the stop-and-go waves that were observed in experiments under laboratory conditions [14,16] have a short pseudoperiod. Hence it is not clear if these waves disappear after a long time or remain. In all cases, their existence has been observed frequently in experiments under laboratory conditions.

We have confirmed the analytical results by simulations which also give information about the nature of the unstable state. These simulations have clearly shown that the unstable regions in the investigated models do not show stop-and-go waves, but instead unrealistic behavior, e.g., backward movement and hence overlapping of pedestrians.

We have discussed that the superposition of forces may lead to negative "desired" speeds and hence to backward movements. In an attempt to avoid this side effect we have introduced a simple force-based model that shows no negative speeds in simulations. As expected, the model is able to produce stop-and-go waves in the instability region instead. However, depending on the chosen values for v'_0, collisions *can* occur, as a result of backwards movement and negative speeds. This is explained by the fact that at the time t_0 when the sum of the repulsive force and the positive driving term vanishes the system is described by the following ODE

$$\ddot{x}'_n + \dot{x}'_n = 0, \tag{35}$$

which yields a speed that decays exponentially:

$$\dot{x}'_n = \dot{x}'_n(t_0)\exp(-t). \tag{36}$$

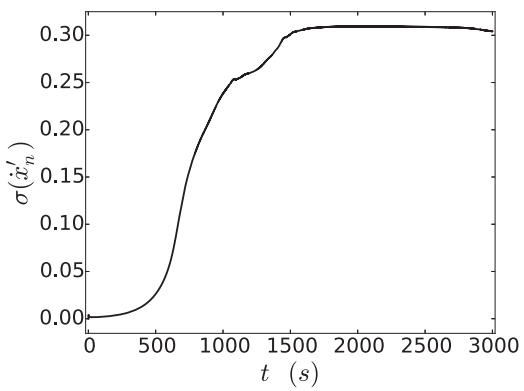

FIG. 13. Standard deviation of the speed with respect to simulation time. The initial perturbation in the speed stabilizes at a nonzero value.

t_0 can be interpreted as the time at which pedestrians start anticipating possible collision. Larger v'_0 implies a slower relaxation of the velocity. Therefore, a possible enhancement of this model could be to shift the minimal distance such that at t_0, $\Delta x'_n \neq 0$. That improves the ability of the system to tolerate slower decay of speeds for $t > t_0$. However, the main difficulty is that the value of the critical time t_0 remains unknown and cannot be easily calculated. This would require adding more complexity to the model, e.g., by considering behavioral anticipation of the dynamics, adding more (physical) forces, or implementing extra collision detection techniques.

The investigations presented here were performed for single-file motion, i.e., a strictly one-dimensional scenario. Although this situation is well studied empirically in several controlled experiments, generically pedestrian dynamics is two dimensional. It remains to be seen, both theoretically and empirically, how the scenario found here changes in this case.

ACKNOWLEDGMENTS

M.C. is grateful to Japan Society for the Promotion of Science (JSPS) for funding this work under Grant No. PE 12078. T.E. acknowledges support from JSPS Grants-in-Aid for Scientific Research (13J05086). A. Sch. thanks the Deutsche Forschungsgemeinschaft (DFG) for support under Grant No. "Scha 636/9-1."

APPENDIX

1. Derivation of stability condition for algebraic forces

Here we give the details of the derivation of the stability criterion of Sec. III B. From (13) we find that

$$\dot{x}_n' = v' + \dot{\epsilon}_n, \quad \Delta\dot{x}_n' = \Delta\dot{\epsilon}_n, \quad \ddot{x}_n' = \ddot{\epsilon}_n, \tag{A1}$$

since $\ddot{y}_n = 0$. Inserting this into the equation of motion (9) we obtain

$$\ddot{\epsilon}_n = -F \cdot G + v_0' - v' - \dot{\epsilon}_n, \tag{A2}$$

where F and G are defined as

$$F = (d' + \Delta\epsilon_n - \tilde{a}_v(\dot{\epsilon}_n + \dot{\epsilon}_{n+1}))^{-q}, \tag{A3}$$

$$G = (\mu + \delta r_\varepsilon(\Delta\dot{\epsilon}_n))^2, \tag{A4}$$

and $d' = \Delta y - 2\tilde{a}_v v' - 2$. We suppose that v and ρ are such that $d' \neq 0$. Considering the first-order approximation of $\exp(x)$ for $x \ll \varepsilon$ we have

$$\begin{aligned} r_\varepsilon(x) &\approx \varepsilon \ln\left(2 - \frac{x}{\varepsilon}\right) = \varepsilon\left(\ln(2) + \ln\left(1 - \frac{x}{2\varepsilon}\right)\right) \\ &\approx \varepsilon \ln(2) - \frac{1}{2}x\,. \end{aligned} \tag{A5}$$

Then,

$$G \approx \left(\mu + \delta\varepsilon \ln(2) - \frac{1}{2}\delta\Delta\dot{\epsilon}_n\right)^2 \approx \gamma^2 - \delta\gamma\Delta\dot{\epsilon}_n, \tag{A6}$$

where we have introduced $\gamma = \mu + \delta\varepsilon \ln(2)$. Using the effective distance Eq. (5), the expression for F can be written as

$$\begin{aligned} F &= \left(\frac{1}{d'}\right)^q \Bigg(1 - \underbrace{\frac{\tilde{a}_v(\dot{\epsilon}_n + \dot{\epsilon}_{n+1}) - \Delta\epsilon_n}{d'}}_{\ll 1}\Bigg)^{-q} \\ &\approx \left(\frac{1}{d'}\right)^q \left(1 + q\frac{\tilde{a}_v(\dot{\epsilon}_n + \dot{\epsilon}_{n+1}) - \Delta\epsilon_n}{d'}\right). \end{aligned} \tag{A7}$$

Substituting the expressions for F and G in Eq. (A2) yields

$$\begin{aligned} \ddot{\epsilon}_n = &-\left(\frac{1}{d'}\right)^q \left(\gamma^2 + \frac{\gamma^2 q\tilde{a}_v}{d'}(\dot{\epsilon}_n + \dot{\epsilon}_{n+1}) - \frac{\gamma^2 q}{d'}\Delta\epsilon_n - \delta\gamma\Delta\dot{\epsilon}_n\right) \\ &+ v_0' - v' - \dot{\epsilon}_n. \end{aligned} \tag{A8}$$

In the steady state the equation of motion (9) simplifies to

$$0 = -\frac{\gamma^2}{d'^q} + v_0' - v', \tag{A9}$$

and we obtain after rearranging Eq. (A8)

$$\ddot{\epsilon}_n = \frac{\delta\gamma}{d'^q}\Delta\dot{\epsilon}_n + \frac{\gamma^2 q}{d'^{q+1}}\Delta\epsilon_n - \frac{\gamma^2 q\tilde{a}_v}{d'^{q+1}}(\dot{\epsilon}_n + \dot{\epsilon}_{n+1}) - \dot{\epsilon}_n. \tag{A10}$$

Assuming a perturbation of the form $\epsilon_n(t) = \alpha_n e^{zt}$ with $z \in \mathbb{C}$ and $\alpha_n \in \mathbb{R}$, $n = 1, \ldots, N$ yields

$$\begin{aligned} \alpha_n z^2 = &\frac{\delta\gamma}{d'^q} z(\alpha_{n+1} - \alpha_n) + \frac{\gamma^2 q}{d'^{q+1}}(\alpha_{n+1} - \alpha_n) \\ &- \frac{\gamma^2 q\tilde{a}_v}{d'^{q+1}} z(\alpha_n + \alpha_{n+1}) - \alpha_n z, \end{aligned} \tag{A11}$$

with $\alpha_{N+1} = \alpha_1$. Introducing

$$\begin{aligned} A &= \frac{\delta\gamma}{d'^q} z + \frac{\gamma^2 q}{d'^{q+1}} - \frac{\gamma^2 q\tilde{a}_v}{d'^{q+1}} z \quad \text{and} \\ B &= z^2 + \frac{\delta\gamma}{d'^q} z + \frac{\gamma^2 q}{d'^{q+1}} + \frac{\gamma^2 q\tilde{a}_v}{d'^{q+1}} z + z, \end{aligned} \tag{A12}$$

Eq. (A11) takes the simple form

$$\alpha_n = \alpha_{n+1}\frac{A}{B}. \tag{A13}$$

Iterating over n, we obtain the rational fraction in z

$$\left(\frac{A}{B}\right)^N = 1 \Leftrightarrow A = Be^{i2\pi l/N}, \quad l = 0, \ldots, N-1. \tag{A14}$$

This equation is

$$z^2 = \delta\gamma\frac{e^{ik} - 1}{d'^q} z - \phi\tilde{a}_v(e^{ik} + 1)z + \phi(e^{ik} - 1) - z, \tag{A15}$$

with $\phi = \frac{q\gamma^2}{d'^{q+1}}$ and $k = 2\pi l/N$ with $l = 0, \ldots, N-1$.

The system described by the equation of motion (9) is stable if the real part $\mathrm{Re}[z]$ of all roots z of Eq. (15) is negative. Let z^+ and z^- be two roots of Eq. (15). For five models (see Table I), we investigate the stability regions in dependence of different wave numbers k and different densities (Fig. 14). Since $z^+ > z^-$ it is enough to check the sign of z^+.

We can observe that introducing a velocity dependence in the form of relative velocity in the numerator of the repulsive term (9) or in the space requirement (3) has a stabilizing effect on the behavior of the model, especially for small wave numbers k.

a. *Stability for small k*

Limiting the expansion to second order and taking advantage of $e^{ik} \approx 1 + ik - \frac{k^2}{2}$ we obtain from Eq. (A15)

$$\begin{aligned} {z^{(0)}}^2 k^2 = &\frac{\delta\gamma}{d'^q}\left(ik - \frac{k^2}{2}\right)(z^{(0)}k + z^{(1)}k^2) + \phi\left(ik - \frac{k^2}{2}\right) \\ &- \tilde{a}_v\phi\left(2 + ik - \frac{k^2}{2}\right)(z^{(0)}k + z^{(1)}k^2) \\ &- (z^{(0)}k + z^{(1)}k^2) \\ = &\left(i\frac{\delta\gamma}{d'^q} z^{(0)} - \frac{\phi}{2} - 2\tilde{a}_v\phi z^{(1)} - i\tilde{a}_v\phi z^{(0)} - z^{(1)}\right)k^2 \\ &+ (i\phi - 2\tilde{a}_v\phi z^{(0)} - z^{(0)})k. \end{aligned} \tag{A16}$$

Rearranging with respect to k yields

$$\begin{aligned} &\left({z^{(0)}}^2 - i\frac{\delta\gamma}{d'^q} z^{(0)} + \frac{\phi}{2} + 2\tilde{a}_v\phi z^{(1)} + i\tilde{a}_v\phi z^{(0)} + z^{(1)}\right)k^2 \\ &- (i\phi - 2\tilde{a}_v\phi z^{(0)} - z^{(0)})k = 0. \end{aligned} \tag{A17}$$

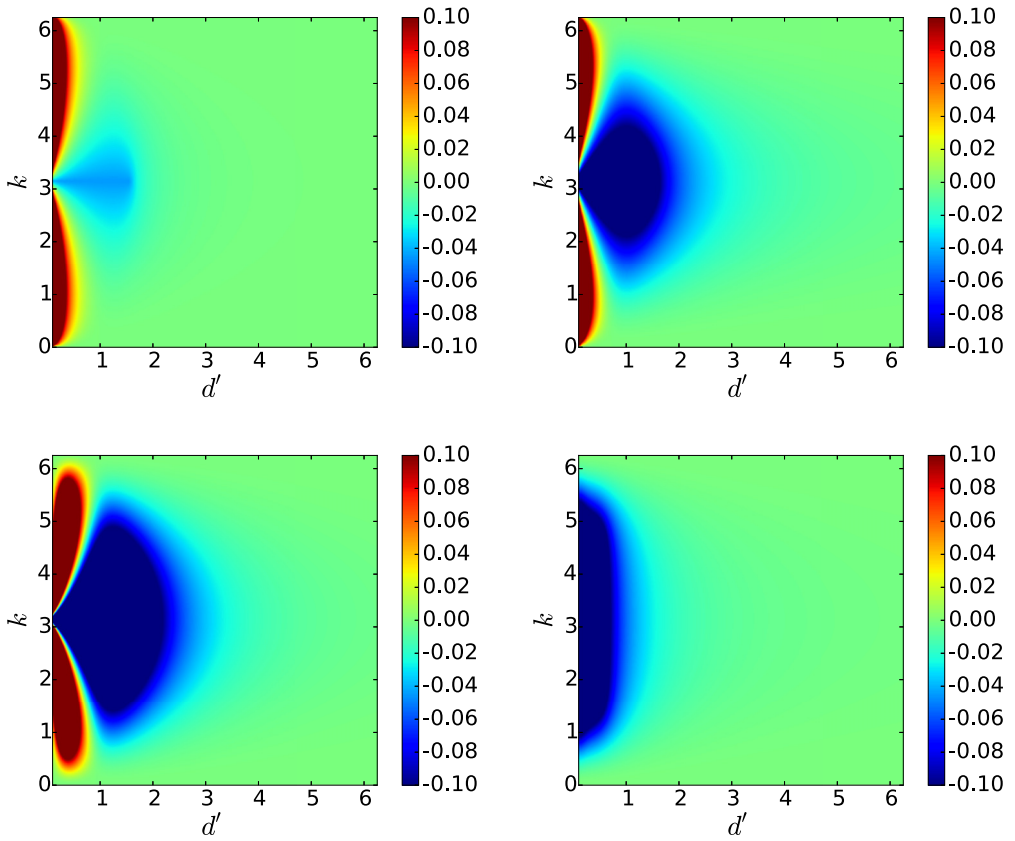

FIG. 14. (Color online) Stability region in the (d',k) space for different model classes. Top left: $\mathcal{Q} = \langle 0.5,0,2,0\rangle$. Top right: $\mathcal{Q} = \langle 0.5,0,1,0\rangle$. Bottom left: $\mathcal{Q} = \langle 0.5,0,2,0.1\rangle$. Bottom right: $\mathcal{Q} = \langle 0.5,1,1,0.1\rangle$. The colors are mapped to the value of $\mathrm{Re}[z^+]$ such that stability corresponds to $\mathrm{Re}[z^+] < 0$.

By a first-order approximation the terms with k^2 in Eq. (A17) can be ignored which leads to

$$i\phi - 2\tilde{a}_v\phi z^{(0)} - z^{(0)} = 0. \tag{A18}$$

Hence

$$z^{(0)} = i\frac{\phi}{2\tilde{a}_v\phi + 1}. \tag{A19}$$

With $\mathrm{Re}[z^{(0)}] = 0$ we notice that a first order approximation is not enough to provide the stability criterion; therefore we consider a second order approximation. From Eq. (A17) and because of Eq. (A18) we obtain

$$z^{(0)2} - i\left(\frac{\delta\gamma}{d'^q} - \tilde{a}_v\phi\right)z^{(0)} + (2\tilde{a}_v\phi + 1)z^{(1)} + \frac{\phi}{2} = 0. \tag{A20}$$

Replacing the expression of $z^{(0)}$ from (A19) in (A20) yields

$$\left(i\frac{\phi}{2\tilde{a}_v\phi + 1}\right)^2 - i\left(\frac{\delta\gamma}{d'^q} - \tilde{a}_v\phi\right)\left(i\frac{\phi}{2\tilde{a}_v\phi + 1}\right) + (2\tilde{a}_v\phi + 1)z^{(1)} + \frac{\phi}{2} = 0, \tag{A21}$$

or

$$\frac{2\tilde{a}_v\phi + 1}{\phi}z^{(1)} = \frac{\phi}{(2\tilde{a}_v\phi + 1)^2} - \left(\frac{\delta\gamma}{d'^q} - \tilde{a}_v\phi\right)\left(\frac{1}{2\tilde{a}_v\phi + 1}\right) - \frac{1}{2}, \quad \phi \neq 0. \tag{A22}$$

Since the coefficient of $z^{(1)}$ is positive, the system described by Eq. (A2) is linearly stable for $k \approx 0$ if

$$\gamma > 0, \quad \phi\omega^2 - \left(\frac{\delta\gamma}{d'^q} - \tilde{a}_v\phi\right)\omega - \frac{1}{2} < 0, \tag{A23}$$

with the following notation: $\omega = \frac{1}{2\tilde{a}_v\phi+1}$. Remarking that $\frac{1}{2}\omega(2\tilde{a}_v\phi + 1) = \frac{1}{2}$, the inequality (A23) can be simplified to

$$\gamma > 0, \quad \Phi := \phi\omega - \frac{\delta\gamma}{d'^q} - \frac{1}{2} < 0. \tag{A24}$$

Here, as a reminder, $\phi = \frac{q\gamma^2}{d'^{q+1}}$, $\gamma = \mu + \delta\varepsilon\ \ln(2)$, and $d' = \Delta y - 2\tilde{a}_v v - 2$, with $\tilde{a}_v = a_v/\tau$. Note that since $\delta,\mu \geqslant 0$ and $\varepsilon > 0$, $\gamma > 0$ implies here $\mu > 0$ or $\delta > 0$.

2. Derivation of stability condition for exponential forces

As in the previous section we add a small dimensionless perturbation ϵ_n to the uniform solution and get from Eq. (19)

$$\ddot{\epsilon}_n = -a\ \exp\left(\frac{-d'}{b}\right)\exp\left(\frac{\tilde{a}_v(\dot{\epsilon}_n + \dot{\epsilon}_{n+1}) - \Delta\epsilon_n}{b}\right) - c\left(\varepsilon\ \ln(2) - \frac{1}{2}(d' + \Delta\epsilon - \tilde{a}_v(\dot{\epsilon}_n + \dot{\epsilon}_{n+1})\right) + v'_0 - v' - \dot{\epsilon}_n. \tag{A25}$$

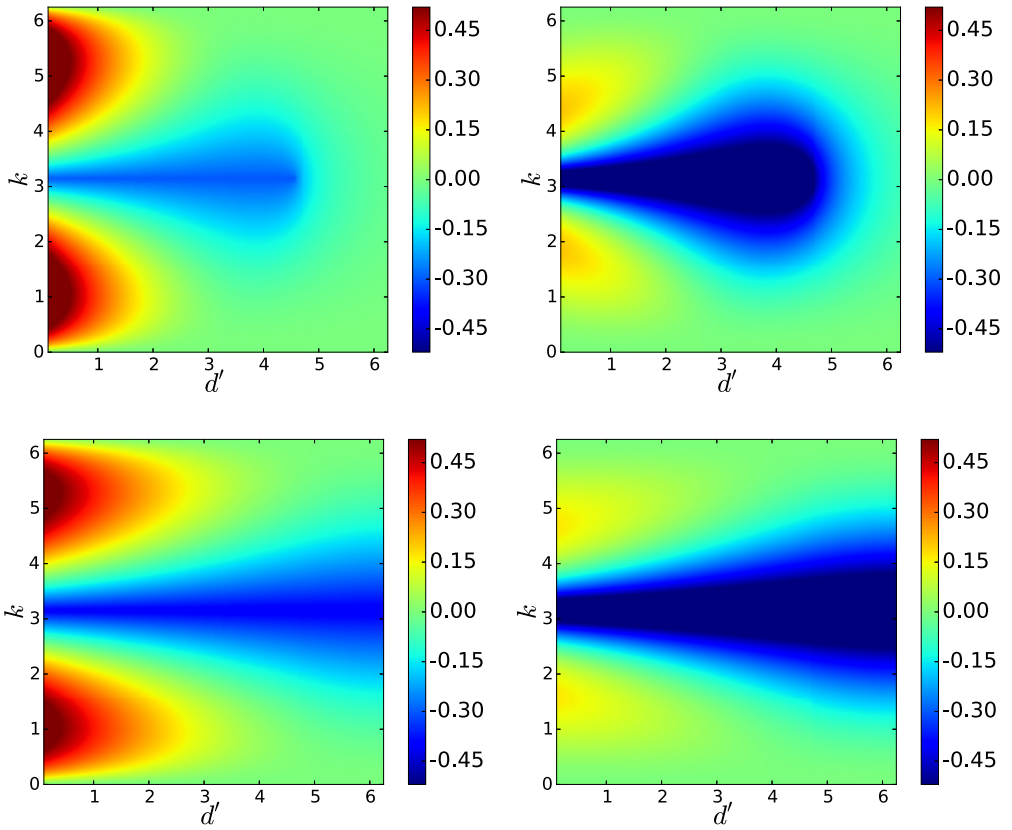

FIG. 15. (Color online) Stability region in the (d',k) space for different model classes. Top left: $\tilde{\mathcal{Q}} = \langle 12,1,0,0\rangle$. Top right: $\tilde{\mathcal{Q}} = \langle 12,1,0,0.2\rangle$. Bottom left: $\tilde{\mathcal{Q}} = \langle 12,2,0,0\rangle$. Bottom right: $\tilde{\mathcal{Q}} = \langle 12,2,0,0.2\rangle$. The colors are mapped to the value of $\mathrm{Re}(\tilde{z}^{+})$.

In the steady state we have $\ddot{x}^{(0)} = 0$ and Eq. (19) reduces to

$$0 = -a\,\exp\left(\frac{-d'}{b}\right) - c\left(\varepsilon\,\ln(2) - \frac{1}{2}d'\right) + v_0' - v'. \quad \text{(A26)}$$

Applying (A26) to (A25) yields

$$\begin{aligned}\ddot{\epsilon}_n &= \underbrace{-a\,\exp\left(\frac{-d'}{b}\right)}_{\tilde{a}}\left(\exp\left(\frac{\tilde{a}_v(\dot{\epsilon}_n + \dot{\epsilon}_{n+1}) - \Delta\epsilon_n}{b}\right) - 1\right)\\ &\quad + \frac{1}{2}c(\Delta\epsilon_n - \tilde{a}_v(\dot{\epsilon}_n + \dot{\epsilon}_{n+1})) - \dot{\epsilon}_n\\ &\approx \tilde{a}\left(\frac{\tilde{a}_v(\dot{\epsilon}_n + \dot{\epsilon}_{n+1}) - \Delta\epsilon_n}{b}\right) + \frac{1}{2}c(\Delta\epsilon_n - \tilde{a}_v(\dot{\epsilon}_n + \dot{\epsilon}_{n+1}))\\ &\quad - \dot{\epsilon}_n\\ &= \tilde{a}_v\left(\tilde{a}/b - \frac{1}{2}c\right)(\dot{\epsilon}_n + \dot{\epsilon}_{n+1}) - \left(\tilde{a}/b - \frac{1}{2}c\right)\Delta\epsilon_n - \dot{\epsilon}_n.\end{aligned} \quad \text{(A27)}$$

By introducing the substitutions $\tilde{c} = \tilde{a}/b - \frac{1}{2}c$ and $\tilde{b} = \tilde{a}_v\tilde{c}$ we obtain a simplified equation for the perturbation:

$$\ddot{\epsilon}_n = \tilde{b}(\dot{\epsilon}_n + \dot{\epsilon}_{n+1}) - \tilde{c}\Delta\epsilon_n - \dot{\epsilon}_n. \quad \text{(A28)}$$

Using the expansion $\epsilon_n(t) = \alpha_n e^{zt}$, we obtain

$$z^2 - (\tilde{b}(e^{ik} + 1) - 1)z + \tilde{c}(e^{ik} - 1) = 0. \quad \text{(A29)}$$

Figure 15 shows the instability regions in the (k,d') space. With $\tilde{a}_v \neq 0$ the instability of the system is considerably reduced.

a. Stability for small k

We further focus on the case $k \approx 0$. For the solution $z \approx z^{(0)}k + z^{(1)}k^2$ we obtain by substituting in (A29)

$$\begin{aligned}z^{(0)^2} &= \tilde{b}\left(2 + ik - \frac{k^2}{2}\right)(z^{(0)}k + z^{(1)}k^2)\\ &\quad - \tilde{c}\left(ik - \frac{k^2}{2}\right) - (z^{(0)}k + z^{(1)}k^2).\end{aligned} \quad \text{(A30)}$$

Rearranging the coefficients of the same power yields

$$\begin{aligned}&\left(-z^{(0)^2} + 2\tilde{b}z^{(1)} + i\tilde{b}z^{(0)} + \frac{\tilde{c}}{2} - z^{(1)}\right)k^2\\ &\quad + (2\tilde{b}z^{(0)} - i\tilde{c} - z^{(0)})k = 0.\end{aligned} \quad \text{(A31)}$$

A first-order approximation yields by ignoring the k^2 term in (A31):

$$z^{(0)} = i\frac{\tilde{c}}{2\tilde{b}\tau - 1}. \quad \text{(A32)}$$

Since $\mathrm{Re}(z^{(0)}) = 0$, we consider a second order approximation of z. Therefore, replacing $z^{(0)}$ by its expression from (A32)

yields

$$z^{(1)}(2\tilde{b}-1) = -\frac{\tilde{c}}{2} - \left(\frac{\tilde{c}}{2\tilde{b}-1}\right)^2 + \tilde{b}\frac{\tilde{c}}{2\tilde{b}-1}. \quad \text{(A33)}$$

Finally, we obtain for $z^{(1)}$

$$\begin{aligned} z^{(1)} &= -\left(\frac{\tilde{c}}{2} + \left(\frac{\tilde{c}}{2\tilde{b}-1}\right)^2 - \tilde{b}\frac{\tilde{c}}{2\tilde{b}-1}\right)\left(\frac{1}{2\tilde{b}-1}\right) \\ &= -\alpha\left(\frac{\tilde{c}}{2} + \tilde{c}^2\alpha^2 - \tilde{b}\tilde{c}\alpha\right). \end{aligned} \quad \text{(A34)}$$

and the system is linearly stable for $k \approx 0$ if

$$-\alpha\left(\frac{\tilde{c}}{2} + \tilde{c}^2\alpha^2 - \tilde{b}\tilde{c}\alpha\right) < 0, \quad \text{(A35)}$$

where $\alpha = \frac{1}{2\tilde{b}-1}$. By simplifying using $-\alpha^2\tilde{c} > 0$, we obtain the condition

$$\tilde{\Phi} = -\frac{1}{2} + \tilde{c}\alpha < 0, \quad \text{(A36)}$$

with $\alpha = \frac{1}{2\tilde{b}-1}$, $\tilde{b} = \tilde{a}_v\tilde{c}$, $\tilde{c} = \tilde{a}/b - \frac{1}{2}c$, and $\tilde{a} = -a\,\exp(-d'/b)$.

[1] D. Helbing, Traffic and related self-driven many-particle systems, Rev. Mod. Phys. **73**, 1067 (2001).

[2] A. Schadschneider, W. Klingsch, H. Klüpfel, T. Kretz, C. Rogsch, and A. Seyfried, *Encyclopedia of Complexity and System Science* (Springer, Berlin, 2009), Vol. 5, pp. 3142–3176.

[3] A. Schadschneider, D. Chowdhury, and K. Nishinari, *Stochastic Transport in Complex Systems. From Molecules to Vehicles* (Elsevier Science Publishing Co Inc., Amsterdam, 2010).

[4] *Modeling, Simulation and Visual Analysis of Crowds A Multidisciplinary Perspective*, edited by S. Ali, K. Nishino, D. Manocha, and M. Shah (Springer, New York, 2013).

[5] A. Seyfried and A. Schadschneider, Fundamental diagram and validation of crowd models, Lect. Notes Comput. Sci. **5191**, 563 (2008).

[6] A. Schadschneider and A. Seyfried, Empirical results for pedestrian dynamics and their implications for cellular automata models, in *Pedestrian Behavior: Data Collection and Applications*, 1st ed., edited by H. Timmermans (Emerald Group Publishing Limited, Bingley, UK, 2009), Chap. 2, pp. 27–43.

[7] Q. Zhang and B. Han, Simulation model of pedestrian interactive behavior, Physica A **390**, 636 (2011).

[8] W. J. Yu, R. Chen, L. Y. Dong, and S. Q. Dai, Centrifugal force model for pedestrian dynamics, Phys. Rev. E **72**, 026112 (2005).

[9] D. Helbing, Collective phenomena and states in traffic and self-driven many-particle systems, Comput. Mater. Sci. **30**, 180 (2004).

[10] T. I. Lakoba, D. J. Kaup, and N. M. Finkelstein, Modifications of the Helbing-Molnár-Farkas-Vicsek social force model for pedestrian evolution, Simulation **81**, 339 (2005).

[11] D. R. Parisi and C. O. Dorso, Morphological and dynamical aspects of the room evacuation process, Physica A **385**, 343 (2007).

[12] A. Garcimartin, I. Zuriguel, J. M. Pastor, C. Martın Gømez, and D. R. Parisi, Experimental evidence of the "faster is slower" effect, Transport. Res. Proc. **2**, 760 (2014).

[13] D. R. Parisi, S. A. Soria, and R. Josens, Faster-is-slower effect in escaping ants revisited: Ants do not behave like humans, Safety Sci. **72**, 274 (2015).

[14] A. Portz and A. Seyfried, Modeling stop-and-go waves in pedestrian dynamics, in *PPAM 2009, Part II*, edited by R. Wyrzykowski, J. Dongarra, K. Karczewski, and J. Wasniewski (Springer, Berlin, 2010), pp. 561–568.

[15] A. Seyfried, A. Portz, and A. Schadschneider, Phase coexistence in congested sates of pedestrian dynamics, Lect. Notes Comput. Sci. **6350**, 496 (2010).

[16] S. Lemercier, A. Jelic, R. Kulpa, J. Hua, J. Fehrenbach, P. Degond, C. Appert-Rolland, S. Donikian, and J. Pettré, Realistic following behaviors for crowd simulation, Comput. Graphics Forum **31**, 489 (2012).

[17] C. Eilhardt and A. Schadschneider, Stochastic headway dependent velocity model for 1d pedestrian dynamics at high densities, Transport. Res. Proc. **2**, 400 (2014).

[18] M. Chraibi, arXiv:1412.1133.

[19] D. Chowdhury, L. Santen, and A. Schadschneider, Statistical physics of vehicular traffic and some related systems, Phys. Rep. **329**, 199 (2000).

[20] D. C. Gazis, The origins of traffic theory, Oper. Res. **50**, 69 (2002).

[21] G. Orosz, R. E. Wilson, and G. Stépán, Traffic jams: Dynamics and control, Phil. Trans. R. Soc. A **368**, 4455 (2010).

[22] T. Nagatani, The physics of traffic jams, Rep. Prog. Phys. **65**, 13 (2002).

[23] G. Köster, F. Treml, and M. Gödel, Avoiding numerical pitfalls in social force models, Phys. Rev. E **87**, 063305 (2013).

[24] M. Chraibi, A. Seyfried, and A. Schadschneider, Quantitative validation of the generalized centrifugal force model, in *Pedestrian and Evacuation Dynamics 2012*, edited by U. Weidmann, U. Kirsch, and M. Schreckenberg (Springer, New York, 2014), pp. 603–613.

[25] M. Chraibi, A. Seyfried, and A. Schadschneider, The generalized centrifugal force model for pedestrian dynamics, Phys. Rev. E **82**, 046111 (2010).

[26] M. Chraibi, U. Kemloh, A. Seyfried, and A. Schadschneider, Force-based models of pedestrian dynamics, Netw. Heterogen. Media **6**, 425 (2011).

[27] J. van den Berg, M. Lin, and D. Manocha, Reciprocal velocity obstacles for real-time multi-agent navigation, in *IEEE International Conference on Robotics and Automation, 2008, ICRA 2008* (IEEE, New York, 2008), pp. 1928–1935.

[28] B. Maury and J. Venel, Handling of contacts on crowd motion simulations, *Traffic and Granular Flow '07* (Springer, New York, 2009).

[29] J. Venel, Integrating strategies in numerical modelling of crowd motion, in *Pedestrian and Evacuation Dynamics 2008*, edited by W. W. F. Klingsch, C. Rogsch, A. Schadschneider, and M. Schreckenberg (Springer, Berlin Heidelberg, 2010).

[30] S. Patil, J. van den Berg, S. Curtis, M. Lin, and D. Manocha, Directing Crowd Simulations Using Navigation Fields, *IEEE*

Transactions On Visualization And Computer Graphics (IEEE, New York, 2010), Vol. 17, pp. 244–254.

[31] F. Dietrich and G. Köster, Gradient navigation model for pedestrian dynamics, Phys. Rev. E **89**, 062801 (2014).

[32] F. Dietrich, G. Köster, M. Seitz, and I. von Sivers, Bridging the gap: From cellular automata to differential equation models for pedestrian dynamics, J. Comput. Sci. **5**, 841 (2014).

[33] E. Kirik and A. Malyshev, On validation of sigmaeva pedestrian evacuation computer simulation module with bottleneck flow, J. Comput. Sci. **5**, 847 (2014).

[34] A. Portz and A. Seyfried, Analyzing stop-and-go waves by experiment and modeling, in *Pedestrian and Evacuation Dynamics 2010*, edited by R. D. Peacock, E. D. Kuligowski, and J. D. Averill (Springer, New York, 2011), pp. 577–586.

[35] U. Weidmann, Transporttechnik der Fussgänger, Technical Report Schriftenreihe des IVT Nr. 90, Institut für Verkehrsplanung, Transporttechnik, Strassen- und Eisenbahnbau, ETH Zürich, ETH Zürich, 1993, 2nd ed.

[36] M. Chraibi, M. Freialdenhoven, A. Schadschneider, and A. Seyfried, Modeling the desired direction in a force-based model for pedestrian dynamics, in *Traffic and Granular Flow'11* (Springer, Berlin, 2013), pp. 263–275.

[37] In GCFM pedestrians are modeled by ellipses with two velocity-dependent semiaxes.

[38] D. Helbing, I. J. Farkas, and T. Vicsek, Freezing by Heating in a Driven Mesoscopic System, Phys. Rev. Lett. **84**, 1240 (2000).

[39] A. Seyfried, B. Steffen, and T. Lippert, Basics of modelling the pedestrian flow, Physica A **368**, 232 (2006).

[40] R.-Y. Guo, S. C. Wong, H.-J. Huang, Z. Peng, and W. H. K. Lam, A microscopic pedestrian-simulation model and its application to intersecting flows, Physica A **389**, 515 (2010).

[41] R.-Y. Guo and T.-Q. Tang, A simulation model for pedestrian flow through walkways with corners, Simul. Model. Practice Theory **21**, 103 (2012).

[42] R. Löhner, On the modelling of pedestrian motion, Appl. Math. Model. **34**, 366 (2010).

[43] N. Shiwakoti, M. Sarvi, G. Rose, and M. Burd, Animal dynamics based approach for modelling pedestrian crowd egress under panic conditions, Transp. Res. B **45**, 1433 (2011).

[44] I. Karamouzas, B. Skinner, and S. J. Guy, A Universal Power Law Governing Pedestrian Interactions, Phys. Rev. Lett. **113**, 238701 (2014).

[45] M. Moussaïd, D. Helbing, and G. Theraulaz, How simple rules determine pedestrian behavior and crowd disasters, Proc. Natl. Acad. Sci. USA **108**, 6884 (2011).

[46] M. Treiber and V. Kanagaraj, Comparing numerical integration schemes for time-continuous car-following models, Physica A (Amsterdam) **419**, 183 (2015).

[47] D. Helbing and P. Molnár, Social force model for pedestrian dynamics, Phys. Rev. E **51**, 4282 (1995).

[48] D. Helbing, I. Farkas, and T. Vicsek, Simulating dynamical features of escape panic, Nature (London) **407**, 487 (2000).

[49] A. Johansson, D. Helbing, and P. K. Shukla, Specification of the social force pedestrian model by evolutionary adjustment to video tracking data, Adv. Complex Syst. **10**, Suppl. No. 2, 271 (2007).

[50] D. R. Parisi, M. Gilman, and H. Moldovan, A modification of the social force model can reproduce experimental data of pedestrian flows in normal conditions, Physica A **388**, 3600 (2009).

[51] M. Moussaïd, D. Helbing, S. Garnier, A. Johansson, M. Combe, and G. Theraulaz, Experimental study of the behavioural mechanisms underlying self-organization in human crowds, Proc. R. Soc. B **276**, 2755 (2009).

[52] D. Helbing, M. Isobe, T. Nagatani, and K. Takimoto, Lattice gas simulation of experimentally studied evacuation dynamics, Phys. Rev. E **67**, 067101 (2003).

[53] M. Bando, K. Hasebe, A. Nakayama, A. Shibata, and Y. Sugiyama, Dynamical model of traffic congestion and numerical simulation, Phys. Rev. E **51**, 1035 (1995).

[54] A. Nakayama, K. Hasebe, and Y. Sugiyama, Instability of pedestrian flow and phase structure in a two-dimensional optimal velocity model, Phys. Rev. E **71**, 036121 (2005).

[55] K. Hirai and K. Tarui, A simulation of the behavior of a crowd in panic, in *Proceedings of the 1975 International Conference on Cybernetics and Society* (Institute of Electrical and Electronics Engineers, New York, 1979), pp. 409–411.

[56] I. Karamouzas, P. Heil, P. van Beek, and M. H. Overmars, A predictive collision avoidance model for pedestrian simulation, Lect. Notes Comput. Sci. **5884**, 41 (2009).